A Dihedral Acute Triangulation of the Cube

Evan VanderZee [*]   Anil N. Hirani [†]   Vadim Zharnitsky [‡]

Damrong Guoy [§]

Abstract

It is shown that there exists a dihedral acute triangulation of the three-dimensional cube. The method of constructing the acute triangulation is described, and symmetries of the triangulation are discussed.

1 Introduction

Interest in acute triangulation of polyhedra dates back to the 1960s at least; when geometers were first working on proving that abstract polyhedra could be realized geometrically, acute triangulations of polyhedra played a role in the solution [5]. In the 1970s, Ciarlet and Raviart showed that a finite element solution of a reaction-diffusion problem satisfies a discrete maximum principle if the triangulation is acute and satisfies some other geometric conditions [7]. Keen interest in acute and nonobtuse triangulations continues today, as evidenced by a recent review article on the subject [3].

The review article poses the specific problem of obtaining dihedral acute triangulations of domains in high-dimensional spaces. The problem also appears in unpublished lecture notes of Pak [10]. Pak mentions that in $\mathbb{R}^5$ and in higher-dimensional spaces, there is no acute triangulation of the hypercube, leaving the proof to the reader. The problem is a combinatorial one, and a proof is given in the literature by Křížek [9]. The acute triangulation of $\mathbb{R}^3$ and of infinite slabs in $\mathbb{R}^3$ was solved by Eppstein, Sullivan, and Üngör [8], who also stated that acute triangulation of the cube is an open problem. Brandts, Korotov, and Křížek mention the problem in a recent paper that improves the results of Ciarlet and Raviart but retains the requirement that the finite element mesh be an acute triangulation [4]. Saraf also indicates that acute triangulation of the cube is an open problem [12].

Acute triangulation can be thought of as an improvement of a nonobtuse triangulation. However, in general acute triangulation is a much more challenging problem than nonobtuse triangulation. As noted above, there is no acute triangulation of the hypercube in $\mathbb{R}^5$ or in higher-dimensional spaces, but there is a nonobtuse triangulation of the hypercube in any dimension [1]. The construction uses path simplices, and the basic idea is to add a main diagonal of the hypercube. This construction works in $\mathbb{R}^3$, as well, producing a nonobtuse triangulation of the cube with six congruent nonobtuse tetrahedra fitting together around a main diagonal.

[*]Department of Mathematics, University of Illinois at Urbana-Champaign (vanderze@illinois.edu)

[†]Department of Computer Science, University of Illinois at Urbana-Champaign (hirani@cs.uiuc.edu)

[‡]Department of Mathematics, University of Illinois at Urbana-Champaign (vz@math.uiuc.edu)

[§]Synopsys Inc. (Damrong.Guoy@synopsys.com)

A nonobtuse triangulation with five tetrahedra is also possible; removing the regular tetrahedron whose vertices are four pairwise nonadjacent corners of the cube leaves four nonobtuse tetrahedra. In contrast, some simple computations with Euler's formula show that any acute triangulation of the cube must have more than 100 tetrahedra.

This paper shows that the cube in $\mathbb{R}^3$ does have an acute triangulation. In fact, it has infinitely many acute triangulations. The acute triangulation described in this paper has 1370 tetrahedra. Details about it are given in Sec. 2, along with some statistics that show the superior quality of the triangulation. The maximum dihedral angle is around $84.65°$, well within the range of acute, and the minimum dihedral angle is a nice $35.89°$. Section 3 describes the computer-assisted construction of this acute triangulation of the cube; a hand construction was combined with mesh optimization to build the mesh. The triangulation has some symmetries, which are discussed in Sec 4. The symmetries greatly reduce the number of distinct tetrahedra from 1370 to 82, and can be used to generate the full set of 277 vertices from just 26 of them.
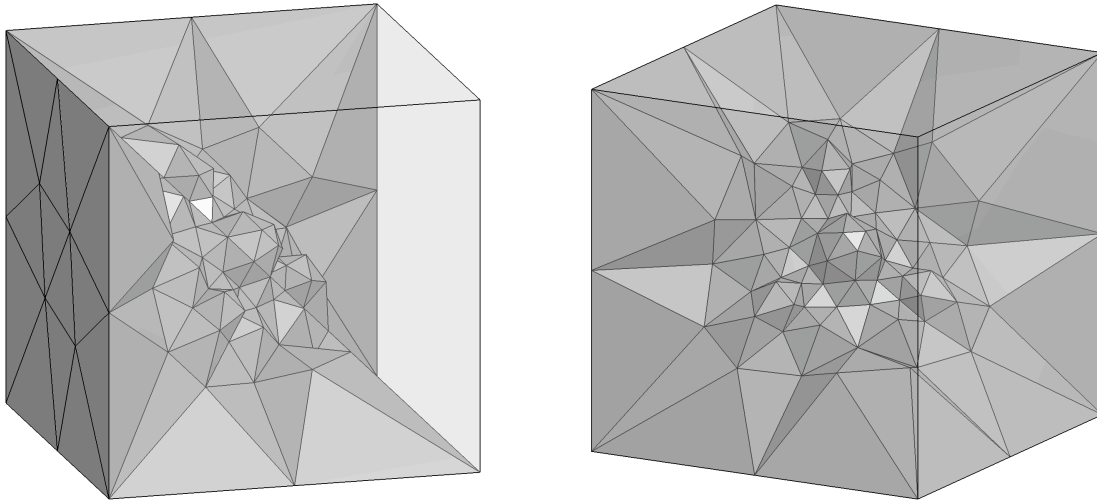
2   The Acute Triangulation

We present the first-known acute triangulation of the cube as a triangulation of a cube centered at the origin with corner vertices at $(\pm 1, \pm 1, \pm 1)$. The coordinates of the vertices of the triangulation are listed in Appendix A. They are also available online, along with code to compute the angles [17]. The mesh connectivity is given by the Delaunay triangulation of the set of vertices. It has been shown that an acute triangulation in three dimensions is not necessarily a Delaunay triangulation [8]. This acute triangulation of the cube, however, is not only Delaunay, but also is one for which each tetrahedron properly contains its circumcenter[1], i.e., the triangulation is 3-well-centered [16].

Figure 1, a cutaway view of the acute triangulation of the cube, visually shows the high quality of the triangulation. Figures 2 through 4 give quantitative evidence of the quality of the triangulation. Each figure is a histogram of some quantitative measurement of the quality of tetrahedra. In each case, the histogram summarizes all of the values of the quantity in the mesh. For instance, the histogram of dihedral angles shows all of the dihedral angles, not just the maximum dihedral angle of each tetrahedron. The h/R values summarized in Fig. 4, which may be less familiar to readers than the other measurements, are related to 3-well-centeredness. The range of the quantity h/R over all tetrahedra is $(-1, 1)$, with 3-well-centered tetrahedra having all values in the range $(0, 1)$. The h/R values in a regular tetrahedron are all $1/3$. See [16] or [14] for more details.

Combinatorics plays an important role in acute triangulation, so we briefly mention some of the combinatorial statistics of the acute triangulation of the cube. There are 277 vertices, 1688 edges, and 1370 tetrahedra. Of the edges, 126 are boundary edges. Of the interior edges, 1506 have the minimum possible number of incident tetrahedra for an acute triangulation, i.e., 5 tetrahedra, and the remaining 56 each have 6 incident tetrahedra. For the vertices, 44 are on the boundary, and 233 are interior. A large majority of the interior vertices (200 of them) have icosahedral neighborhoods, thus they have 12 incident edges. There are 10 vertices with 14 incident edges, 18 vertices with 15 incident edges, 4 vertices with 16 incident edges, and 1 vertex—the central vertex located at $(0, 0, 0)$—with 22 incident edges.

---

[1]This property does not hold in general for acute triangulations. For a tetrahedral mesh in $\mathbb{R}^3$, if each tetrahedron contains its circumcenter, the mesh must be Delaunay [11] [13] [16], so any non-Delaunay acute triangulation does not have this property.

Figure 1: Two views of a cutaway section of the first-known acute triangulation of the cube. The view at right is a $45°$ rotation about the z-axis from the view at left. On the left a 14-triangle triangulation of one of the square faces of the cube is visible. This 14-triangle triangulation of the square is used on each face of the cube.
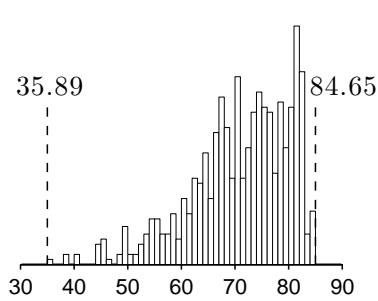
Figure 2: A histogram of the dihedral angles of the acute triangulation of the cube.
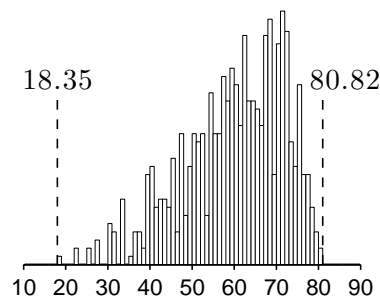
Figure 3: A histogram of the face angles of the acute triangulation of the cube.
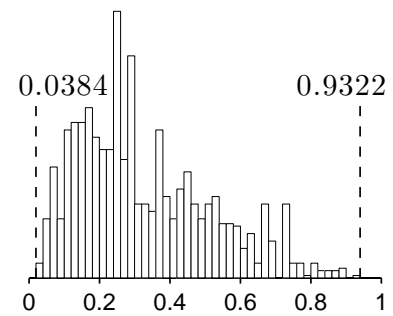
Figure 4: A histogram of the tetrahedron h/R values of the acute triangulation of the cube.

The high degree central vertex can be replaced with a regular tetrahedron to give a combinatorially different acute triangulation of the cube, one with 1387 tetrahedra. To obtain this triangulation, replace the vertex at the origin with the four vertices at $(-0.05, -0.05, 0.05)$, $(-0.05, 0.05, -0.05)$, $(0.05, -0.05, -0.05)$, and $(0.05, 0.05, 0.05)$ and compute the Delaunay triangulation of the new vertex set. The result is acute and completely well-centered. We see that there are at least two combinatorially distinct acute triangulations of the cube conforming to the same surface triangulation.

3   Method of Construction

The basic methodology for the construction was one of an advancing front. It is absolutely necessary to have an acute surface triangulation, since an acute tetrahedron has acute facets [8], and more generally, all facets of an acute simplex are acute [2]. We began with a high-quality acute surface triangulation of the cube; the midpoint of each edge of the cube was added, and each face was triangulated with a 14-triangle acute triangulation that conforms to this boundary and has a maximum face angle around $73.3°$. On the left side of Fig. 1 one can see a 14-triangle acute triangulation of the square on one of the faces of the cube.

Starting from the acute surface triangulation, we built inward, carefully adding vertices and tetrahedra to satisfy the combinatorial constraints. That is, each edge of the triangulation coinciding with an edge of the cube must have at least two incident tetrahedra, each edge of the triangulation lying in a facet of the cube must have at least three incident tetrahedra, and each interior edge must have at least five incident tetrahedra. The addition of vertices and tetrahedra was performed by hand with the frequent computation of the Delaunay triangulation to help get the proper mesh connectivity.

After each layer or partial layer was constructed by hand, the mesh was optimized to obtain a set of acute tetrahedra conforming to the boundary of the cube. The optimization did not explicitly seek a dihedral acute triangulation, but instead tried to make the meshes completely well-centered. (This type of optimization was introduced for two dimensions in [15] and later generalized to higher dimensions in [16].) At each layer, a moderately aggressive version of the optimization yielded a mesh that was both completely well-centered and dihedral acute. In most cases, more aggressive optimization produced a mesh that was well-centered but not acute, and less aggressive optimization produced a mesh that was neither well-centered nor acute. When a dihedral acute and completely well-centered mesh was obtained from the optimization, a new layer consisting of more tetrahedra and vertices was added by hand.

Eventually this process reached a stage in which all of the edges on the internal boundary already had three incident tetrahedra. This and the rest of the combinatorics and geometry worked out so that adding a vertex at the center of the cube and computing the Delaunay triangulation produced an acute, completely well-centered triangulation of the cube.

When the acute triangulation was first obtained and optimized relative to a cost function based on well-centeredness, it had a maximum dihedral angle around $87.8°$. Later some additional optimization was applied that directly optimized the dihedral angle as well as optimizing for well-centeredness, and the symmetry discussed in the next section was enforced exactly. The additional optimization allowed boundary vertices to move constrained to the surfaces of the cube. This optimization produced the final mesh presented in this paper, except that the vertices were rounded to the nearest .001 for ease of presentation.

4 Symmetries of the Triangulation

The acute triangulation of the cube presented in this paper has an S_4 symmetry group. More precisely, it has all of the symmetries of a regular tetrahedron whose vertices are four pairwise nonadjacent corners of the cube. Consider, for instance, the regular tetrahedron with vertices $(-1, -1, -1)$, $(-1, 1, 1)$, $(1, -1, 1)$, and $(1, 1, -1)$. Each of the 24 symmetries of this regular tetrahedron—rotations or reflections in $\mathbb{R}^3$ that map the tetrahedron to itself—is a symmetry that maps this acute triangulation of the cube to itself.

In fact, it is possible to use these symmetries to construct the full set of 277 vertices from just 26 of them. There are multiple ways to do this, one of which is the following. Take the 26 vertices in the list in Table 1 in Appendix A. These 26 vertices are the vertices that lie in the $1/24$th of the cube specified by the inequalities $y \geq -1$, $x \geq y$, $x \leq z$, and $x \leq -z$.

We will transform this initial set of vertices using the orthogonal matrices

$$A_1 = \begin{bmatrix} 0 & 0 & -1 \\ 0 & 1 & 0 \\ -1 & 0 & 0 \end{bmatrix} \quad A_2 = \begin{bmatrix} 0 & 0 & 1 \\ 0 & 1 & 0 \\ 1 & 0 & 0 \end{bmatrix} \quad A_3 = \begin{bmatrix} -1 & 0 & 0 \\ 0 & -1 & 0 \\ 0 & 0 & 1 \end{bmatrix} \quad A_4 = \begin{bmatrix} 0 & 1 & 0 \\ 0 & 0 & 1 \\ 1 & 0 & 0 \end{bmatrix}.$$

Each of these matrices is a symmetry of the aforementioned regular tetrahedron and a symmetry of the cube. Matrix A_1 is a reflection through the plane $x = -z$. Matrix A_2 is a reflection through the plane $x = z$. Matrix A_3 is a $180°$ rotation about the z-axis, which could also be thought of as reflection through the z-axis. Finally, A_4 is a rotation about the main diagonal of the cube passing through $(-1, -1, -1)$ and $(1, 1, 1)$. Looking along this diagonal from $(-1, -1, -1)$ towards $(1, 1, 1)$, the rotation is $120°$ counterclockwise.

Figure 5 shows how these symmetries fill the cube starting from the generating $1/24$th section of the cube. Taking the initial set of 26 vertices that lie in the generating section of the cube, we apply matrix A_1 to obtain a set of vertices that lie in $1/12$th of the cube. Then we apply A_2 to the new vertex set, obtaining a set of vertices lying in $1/6$th of the cube. The region containing the vertices is now a pyramid over the face $y = -1$ with apex at the origin. (Top right in Fig. 5.) To this vertex set we apply A_3 and cover $1/3$rd of the cube. Finally we apply both A_4 and A_4^2—rotating by both $120°$ and $240°$ about a main diagonal—to obtain a set of vertices that covers the full cube. A large number of vertices in this vertex set are duplicates of each other, but when all of the duplicates are removed, there are 277 vertices that remain. The listing of vertex coordinates in Appendix A is divided into separate tables according to the way these symmetries generate the full set of vertices.

Because of the symmetries of this acute triangulation of the cube, there are only 82 distinct tetrahedra used in the 1370-tetrahedron acute triangulation of the cube. The cutaway views of the acute triangulation of the cube in Fig. 6 show just one of each of these 82 tetrahedra as they fit together to cover the generating $1/24$th section of the cube. It is clear from Fig. 6 that many of the tetrahedra do not align with the boundaries of the generating $1/24$th section of the cube. Tetrahedra that intersect the boundaries of the generating region are mapped onto themselves by one or more of the symmetries. In fact, there are only 38 tetrahedra that are interior to the generating section of the cube. There are, of course, 24 copies of each of these tetrahedra in the final result. As far as the other tetrahedra in the generating set are concerned, 35 of them intersect one of the planes bounding the region, 8 of them intersect one of the main diagonals of the cube, and 1 intersects the y-axis. With some thought about the symmetries involved, one can see that in the full acute triangulation of the cube there are 12 copies of each tetrahedron that intersect a plane, 4 copies of each tetrahedron that intersect a main diagonal, and 6 copies of the tetrahedron that intersects the y-axis.

5
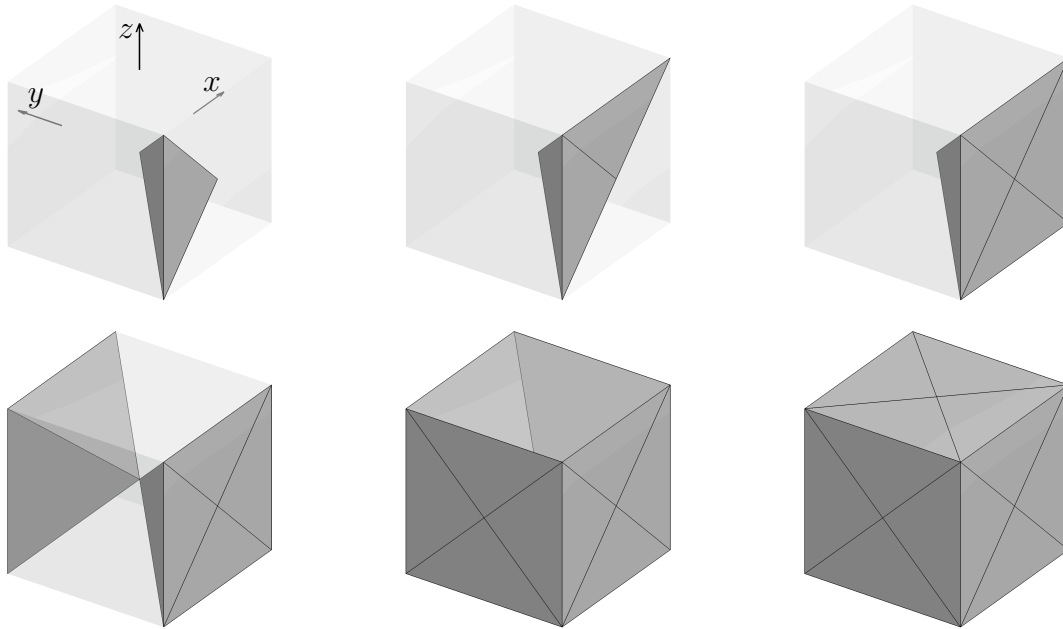
Figure 5: Starting from a set of 26 vertices lying in $1/24$th of the cube, the full set of 277 vertices can be generated using symmetries of the acute triangulation of the cube. This figure shows one way that the symmetries can be used to generate the full vertex set. Starting from the $1/24$th of the cube bounded by the planes $y = -1$, $x = y$, $x = z$, and $x = -z$ (top left), one can fill the cube by performing the following steps in order. Reflect across the plane $x = -z$ (top center). Reflect across the plane $x = z$ (top right). Rotate by $180°$ about the z-axis (bottom left). Simultaneously rotate by $120°$ (bottom center) and $240°$ (bottom right) about the main diagonal through $(-1, -1, -1)$ and $(1, 1, 1)$.

Figure 6: Two views of a cutaway section of the acute triangulation of the cube. The view at right is a $90°$ rotation about the z-axis from the view at left. On the left four of the triangles on the surface of the cube are visible. These triangles appear on the back face of the cube in the view on the right. This cutaway is a collection of one of each of the 82 distinct tetrahedra that are used in the acute triangulation. The tetrahedra fit together to cover a symmetry region, and through rotations and reflections they can generate the full acute triangulation of the cube.

6

5 Conclusions

We have demonstrated that there exists an acute triangulation of the cube. The fact that the cube has an acute triangulation directly implies that many other regions of $\mathbb{R}^3$ also have acute triangulations. In particular, one can reflect the acute triangulation of the cube through one of its faces to get an acute triangulation of a square prism twice as long as a cube with vertices that match on the two square faces. By identifying the matching vertices with each other one can get an acute triangulation of a periodic domain. Alternatively, one can stack infinitely many of these objects together to obtain an acute triangulation of an infinitely long square prism. Using reflections and translations of this acute triangulation, one can easily obtain an acute triangulation of an infinite slab in $\mathbb{R}^3$, or of all of $\mathbb{R}^3$, as alternatives to the constructions in [8]. In fact, one can use translations and reflections of an initial acute triangulation of the cube to acutely triangulate any object in $\mathbb{R}^3$ that can be tiled with cubes. This can be used to create an infinite variety of acute triangulations of the cube itself.

But does every polyhedron have a dihedral acute triangulation? This remains an open question. Does every tetrahedron have a dihedral acute triangulation? This question, too, remains open, and so far there is still no nontrivial acute triangulation of the regular tetrahedron that is known to the authors. It is likely that a computer-assisted construction like the one discussed in this paper could be used to obtain such an acute triangulation, but there may be more direct methods. A directly constructive, perhaps simpler, acute triangulation of the cube would also be of interest.

Another open problem is that of finding the smallest possible acute triangulation of the cube, where size is measured in terms of the number of tetrahedra. It may be that the 1370 tetrahedra acute triangulation presented here is the smallest acute triangulation of the cube possible, but the authors suspect this is not the case. The analogous question in two dimensions—the smallest acute triangulation of the square—has been answered; an acute triangulation of the square requires at least eight triangles [6].

Acknowledgement

References

[1] BERN, M., CHEW, P., EPPSTEIN, D., AND RUPPERT, J. Dihedral bounds for mesh generation in high dimensions. In *SODA '95: Proceedings of the sixth annual ACM-SIAM symposium on discrete algorithms* (Philadelphia, PA, USA, 1995), Society for Industrial and Applied Mathematics, pp. 189–196.

[2] BRANDTS, J., KOROTOV, S., AND KŘÍŽEK, M. Dissection of the path-simplex in $\mathbb{R}^n$ into n path-subsimplices. *Linear Algebra and its Applications 421*, 2–3 (March 2007), 382–393. `doi:10.1016/j.laa.2006.10.010`.

[3] BRANDTS, J., KOROTOV, S., KŘÍŽEK, M., AND ŠOLC, J. On nonobtuse simplicial partitions. *SIAM Review 51*, 2 (2009), 317–335. URL http://link.aip.org/link/?SIR/51/317/1, doi:10.1137/060669073.

[4] BRANDTS, J. H., KOROTOV, S., AND KŘÍŽEK, M. The discrete maximum principle for linear simplicial finite element approximations of a reaction-diffusion problem. *Linear Algebra and its Applications 429*, 10 (2008), 2344 – 2357. Special Issue in honor of Richard S. Varga. URL http://www.sciencedirect.com/science/article/B6V0R-4T2S02T-2/2/40a03300493ca05268aaf67c2f963a43, doi:10.1016/j.laa.2008.06.011.

[5] BURAGO, J. D., AND ZALGALLER, V. A. Polyhedral embedding of a net. *Vestnik Leningrad. Univ. 15*, 7 (1960), 66–80.

[6] CASSIDY, C., AND LORD, G. A square acutely triangulated. *J. Recreational Math 13* (1980/81), 263–268.

[7] CIARLET, P. G., AND RAVIART, P.-A. Maximum principle and uniform convergence for the finite element method. *Computer Methods in Applied Mechanics and Engineering 2*, 1 (February 1973), 17–31. URL http://dx.doi.org/10.1016/0045-7825(73)90019-4, doi:10.1016/0045-7825(73)90019-4.

[8] EPPSTEIN, D., SULLIVAN, J. M., AND ÜNGÖR, A. Tiling space and slabs with acute tetrahedra. *Computational Geometry: Theory and Applications 27*, 3 (2004), 237–255. doi:10.1016/j.comgeo.2003.11.003.

[9] KŘÍŽEK, M. There is no face-to-face partition of $\mathbb{R}^5$ into acute simplices. *Discrete and Computational Geometry 36*, 2 (September 2006), 381–390. doi:10.1007/s00454-006-1244-0.

[10] PAK, I. Lectures on discrete and polyhedral geometry [online]. Unpublished. URL http://www.math.umn.edu/~pak/book.htm [cited 2009].

[11] RAJAN, V. Optimality of the Delaunay triangulation in $\mathbb{R}^d$. *Discrete and Computational Geometry 12*, 1 (December 1994), 189–202. doi:10.1007/BF02574375.

[12] SARAF, S. Acute and nonobtuse triangulations of polyhedral surfaces. *European Journal of Combinatorics 30*, 4 (2009), 833–840. doi:10.1016/j.ejc.2008.08.004.

[13] SCHMITT, D., AND SPEHNER, J.-C. Angular properties of Delaunay diagrams in any dimension. *Discrete and Computational Geometry 21*, 1 (January 1999), 17–36. doi:10.1007/PL00009407.

[14] VANDERZEE, E., HIRANI, A. N., AND GUOY, D. Triangulation of simple 3D shapes with well-centered tetrahedra. In *Proceedings of the 17th International Meshing Roundtable*, R. V. Garimella, Ed. Springer Berlin Heidelberg, Pittsburgh, Pennsylvania, October 12–15 2008, pp. 19–35. Also available as a preprint arXiv:0806.2332v2 [cs.CG] on arxiv.org. doi:10.1007/978-3-540-87921-3_2.

[15] VANDERZEE, E., HIRANI, A. N., GUOY, D., AND RAMOS, E. Well-centered planar triangulation – an iterative approach. In *Proceedings of the 16th International Meshing Roundtable* (Seattle, Washington, October 14–17 2007), M. L. Brewer and D. Marcum, Eds., Springer, pp. 121–138. doi:10.1007/978-3-540-75103-8_7.

[16] VANDERZEE, E., HIRANI, A. N., GUOY, D., AND RAMOS, E. Well-centered triangulation. Tech. Rep. UIUCDCS-R-2008-2936, Department of Computer Science, University of Illinois at Urbana-Champaign, February 2008. Also available as a preprint at arXiv as arXiv:0802.2108v2 [cs.CG]. URL http://arxiv.org/abs/0802.2108.

[17] VANDERZEE, E., HIRANI, A. N., ZHARNITSKY, V., AND GUOY, D. Supplemental data and programs for dihedral acute triangulation of the cube. URL http://www.cs.uiuc.edu/hirani/papers/supplement/acutecube/index.html [cited May 29, 2009].

A   Vertex Coordinates

The coordinates of the vertices of an acute triangulation of the cube are listed in Tables 1 through 6. The full set of vertices is the union of the vertices listed in the individual tables; the tables separate the vertices according to the way they are generated from the symmetries described in Sec. 4.

Table 1: Coordinates of the 26 vertices in the generating section of the cube.

x	y	z
-1	-1	-1
-0.24	-1	-0.24
-1	-1	0
-0.347	-1	0.347
-1	-1	1
-0.517	-0.517	-0.23
-0.559	-0.559	0.357
-0.122	-0.624	0.122
-0.399	-0.598	0.052

x	y	z
-0.152	-0.472	-0.152
-0.27	-0.523	0.27
-0.254	-0.254	-0.254
-0.336	-0.336	0.336
-0.325	-0.325	-0.02
-0.376	-0.376	0.18
0	-0.388	0
-0.21	-0.398	0.099
-0.224	-0.316	0.224

x	y	z
-0.127	-0.269	0.127
-0.158	-0.263	-0.027
-0.2	-0.2	0.2
-0.258	-0.258	0.115
-0.115	-0.115	-0.115
0	-0.214	0
-0.15	-0.15	0.061
0	0	0

Table 2: Coordinates of the 15 new vertices obtained by applying matrix A_1 to the vertices in Table 1.

x	y	z
1	-1	1
0.24	-1	0.24
0	-1	1
0.23	-0.517	0.517
-0.357	-0.559	0.559

x	y	z
-0.052	-0.598	0.399
0.152	-0.472	0.152
0.254	-0.254	0.254
0.02	-0.325	0.325
-0.18	-0.376	0.376

x	y	z
-0.099	-0.398	0.21
0.027	-0.263	0.158
-0.115	-0.258	0.258
0.115	-0.115	0.115
-0.061	-0.15	0.15

Table 3: Coordinates of the 28 new vertices obtained by applying matrix A_2 to the vertices in Tables 1 and 2.

x	y	z
0	-1	-1
0.347	-1	-0.347
1	-1	-1
-0.23	-0.517	-0.517
0.357	-0.559	-0.559
0.122	-0.624	-0.122
0.052	-0.598	-0.399
0.27	-0.523	-0.27
0.336	-0.336	-0.336
-0.02	-0.325	-0.325

x	y	z
0.18	-0.376	-0.376
0.099	-0.398	-0.21
0.224	-0.316	-0.224
0.127	-0.269	-0.127
-0.027	-0.263	-0.158
0.2	-0.2	-0.2
0.115	-0.258	-0.258
0.061	-0.15	-0.15
1	-1	0

x	y	z
0.517	-0.517	0.23
0.559	-0.559	-0.357
0.399	-0.598	-0.052
0.325	-0.325	0.02
0.376	-0.376	-0.18
0.21	-0.398	-0.099
0.158	-0.263	0.027
0.258	-0.258	-0.115
0.15	-0.15	-0.061

Table 4: Coordinates of the 68 new vertices obtained by applying matrix A_3 to the vertices in Tables 1 through 3.

x	y	z
1	1	-1
0.24	1	-0.24
1	1	0
0.347	1	0.347
1	1	1
0.517	0.517	-0.23
0.559	0.559	0.357
0.122	0.624	0.122
0.399	0.598	0.052
0.152	0.472	-0.152
0.27	0.523	0.27
0.254	0.254	-0.254
0.336	0.336	0.336
0.325	0.325	-0.02
0.376	0.376	0.18
0	0.388	0
0.21	0.398	0.099
0.224	0.316	0.224
0.127	0.269	0.127
0.158	0.263	-0.027
0.2	0.2	0.2
0.258	0.258	0.115
0.115	0.115	-0.115

x	y	z
0	0.214	0
0.15	0.15	0.061
-1	1	1
-0.24	1	0.24
0	1	1
-0.23	0.517	0.517
0.357	0.559	0.559
0.052	0.598	0.399
-0.152	0.472	0.152
-0.254	0.254	0.254
-0.02	0.325	0.325
0.18	0.376	0.376
0.099	0.398	0.21
-0.027	0.263	0.158
0.115	0.258	0.258
-0.115	0.115	0.115
0.061	0.15	0.15
0	1	-1
-0.347	1	-0.347
-1	1	-1
0.23	0.517	-0.517
-0.357	0.559	-0.559
-0.122	0.624	-0.122

x	y	z
-0.052	0.598	-0.399
-0.27	0.523	-0.27
-0.336	0.336	-0.336
0.02	0.325	-0.325
-0.18	0.376	-0.376
-0.099	0.398	-0.21
-0.224	0.316	-0.224
-0.127	0.269	-0.127
0.027	0.263	-0.158
-0.2	0.2	-0.2
-0.115	0.258	-0.258
-0.061	0.15	-0.15
-1	1	0
-0.517	0.517	0.23
-0.559	0.559	-0.357
-0.399	0.598	-0.052
-0.325	0.325	0.02
-0.376	0.376	-0.18
-0.21	0.398	-0.099
-0.158	0.263	0.027
-0.258	0.258	-0.115
-0.15	0.15	-0.061

Table 5: Coordinates of the 84 new vertices obtained by applying matrix A_4 to the vertices in Tables 1 through 4.

x	y	z
-1	-0.24	-0.24
-1	0	-1
-1	0.347	-0.347
-0.517	-0.23	-0.517
-0.559	0.357	-0.559
-0.624	0.122	-0.122
-0.598	0.052	-0.399
-0.472	-0.152	-0.152
-0.523	0.27	-0.27
-0.325	-0.02	-0.325
-0.376	0.18	-0.376
-0.388	0	0
-0.398	0.099	-0.21
-0.316	0.224	-0.224
-0.269	0.127	-0.127
-0.263	-0.027	-0.158
-0.258	0.115	-0.258
-0.214	0	0
-0.15	0.061	-0.15
-1	0.24	0.24
-0.598	0.399	-0.052
-0.472	0.152	0.152
-0.398	0.21	-0.099
-0.263	0.158	0.027
-1	-0.347	0.347
-0.624	-0.122	0.122
-0.598	-0.399	0.052
-0.523	-0.27	0.27

x	y	z
-0.398	-0.21	0.099
-0.316	-0.224	0.224
-0.269	-0.127	0.127
-0.263	-0.158	-0.027
-1	0	1
-0.517	0.23	0.517
-0.559	-0.357	0.559
-0.598	-0.052	0.399
-0.325	0.02	0.325
-0.376	-0.18	0.376
-0.398	-0.099	0.21
-0.263	0.027	0.158
-0.258	-0.115	0.258
-0.15	-0.061	0.15
1	-0.24	0.24
1	0	1
1	0.347	0.347
0.517	-0.23	0.517
0.559	0.357	0.559
0.624	0.122	0.122
0.598	0.052	0.399
0.472	-0.152	0.152
0.523	0.27	0.27
0.325	-0.02	0.325
0.376	0.18	0.376
0.388	0	0
0.398	0.099	0.21
0.316	0.224	0.224

x	y	z
0.269	0.127	0.127
0.263	-0.027	0.158
0.258	0.115	0.258
0.214	0	0
0.15	0.061	0.15
1	0.24	-0.24
0.598	0.399	0.052
0.472	0.152	-0.152
0.398	0.21	0.099
0.263	0.158	-0.027
1	-0.347	-0.347
0.624	-0.122	-0.122
0.598	-0.399	-0.052
0.523	-0.27	-0.27
0.398	-0.21	-0.099
0.316	-0.224	-0.224
0.269	-0.127	-0.127
0.263	-0.158	0.027
1	0	-1
0.517	0.23	-0.517
0.559	-0.357	-0.559
0.598	-0.052	-0.399
0.325	0.02	-0.325
0.376	-0.18	-0.376
0.398	-0.099	-0.21
0.263	0.027	-0.158
0.258	-0.115	-0.258
0.15	-0.061	-0.15

Table 6: Coordinates of the 56 new vertices obtained by applying matrix A_4^2 to the vertices in Tables 1 through 4. Vertices that would be duplicated in Table 5 have also been removed.

x	y	z
-0.24	-0.24	-1
0.347	-0.347	-1
0.122	-0.122	-0.624
0.052	-0.399	-0.598
-0.152	-0.152	-0.472
0.27	-0.27	-0.523
0	0	-0.388
0.099	-0.21	-0.398
0.224	-0.224	-0.316
0.127	-0.127	-0.269
-0.027	-0.158	-0.263
0	0	-0.214
0.24	0.24	-1
0.399	-0.052	-0.598
0.152	0.152	-0.472
0.21	-0.099	-0.398
0.158	0.027	-0.263
-0.347	0.347	-1
-0.122	0.122	-0.624

x	y	z
-0.399	0.052	-0.598
-0.27	0.27	-0.523
-0.21	0.099	-0.398
-0.224	0.224	-0.316
-0.127	0.127	-0.269
-0.158	-0.027	-0.263
-0.052	0.399	-0.598
-0.099	0.21	-0.398
0.027	0.158	-0.263
-0.24	0.24	1
0.347	0.347	1
0.122	0.122	0.624
0.052	0.399	0.598
-0.152	0.152	0.472
0.27	0.27	0.523
0	0	0.388
0.099	0.21	0.398
0.224	0.224	0.316
0.127	0.127	0.269

x	y	z
-0.027	0.158	0.263
0	0	0.214
0.24	-0.24	1
0.399	0.052	0.598
0.152	-0.152	0.472
0.21	0.099	0.398
0.158	-0.027	0.263
-0.347	-0.347	1
-0.122	-0.122	0.624
-0.399	-0.052	0.598
-0.27	-0.27	0.523
-0.21	-0.099	0.398
-0.224	-0.224	0.316
-0.127	-0.127	0.269
-0.158	0.027	0.263
-0.052	-0.399	0.598
-0.099	-0.21	0.398
0.027	-0.158	0.263